

Tunable subdiffusion in the Caputo fractional standard map

J. A. Méndez-Bermúdez

Instituto de Física, Benemérita Universidad Autónoma de Puebla, Puebla 72570, Mexico

R. Aguilar-Sánchez

Facultad de Ciencias Químicas, Benemérita Universidad Autónoma de Puebla, Puebla 72570, Mexico

The Caputo fractional standard map (C-fSM) is a two-dimensional nonlinear map with memory given in action-angle variables (I, θ) . It is parameterized by K and $\alpha \in (1, 2]$ which control the strength of nonlinearity and the fractional order of the Caputo derivative, respectively. In this work we perform a scaling study of the average squared action $\langle I^2 \rangle$ along strongly chaotic orbits, i.e. when $K \gg 1$. We numerically prove that $\langle I^2 \rangle \propto n^\mu$ with $0 \leq \mu(\alpha) \leq 1$, for large enough discrete times n . That is, we demonstrate that the C-fSM displays subdiffusion for $1 < \alpha < 2$. Specifically, we show that diffusion is suppressed for $\alpha \rightarrow 1$ since $\mu(1) = 0$, while standard diffusion is recovered for $\alpha = 2$ where $\mu(2) = 1$. We describe our numerical results with a phenomenological analytical estimation. We also contrast the C-fSM with the Riemann-Liouville fSM and Chirikov's standard map.

PACS numbers:

I. PRELIMINARIES

By replacing the second order derivative in the equation of motion of the kicked rotor

$$\frac{d^2\theta}{dt^2} + K \sin(\theta) \sum_{j=0}^{\infty} \delta\left(\frac{t}{T} - j\right) = 0 \quad (1)$$

by fractional operators (fractional derivatives, fractional integrals or fractional integro-differential operators), fractional versions of the kicked rotor are obtained. The kicked rotor represents a free rotating stick in an inhomogeneous field that is periodically switched on in instantaneous pulses, see e.g. [1]. In Eq. (1), $\theta \in [0, 2\pi]$ is the angular position of the stick, K is the kicking strength, T is the kicking period, and δ is Dirac's delta function. Among the several fractional kicked rotors (fKRs) reported in the literature we can mention: the Riemann-Liouville fKR [2, 3]

$${}_0D_t^\alpha \theta + K \sin(\theta) \sum_{j=0}^{\infty} \delta\left(\frac{t}{T} - (j + \epsilon)\right) = 0, \quad 1 < \alpha \leq 2, \quad (2)$$

where $\epsilon \rightarrow 0+$, the Caputo fKR [4, 5]

$${}_0^C D_t^\alpha \theta + K \sin(\theta) \sum_{j=0}^{\infty} \delta\left(\frac{t}{T} - (j + \epsilon)\right) = 0, \quad 1 < \alpha \leq 2, \quad (3)$$

where $\epsilon \rightarrow 0+$, the Hadamard fKR [6], the Erdelyi-Kober fKR [7], and the Hilfer fKR [8]. Above [9, 10],

$$\begin{aligned} {}_0D_t^\alpha \theta(t) &= D_t^m {}_0\mathcal{I}_t^{m-\alpha} \theta(t) \\ &= \frac{1}{\Gamma(m-\alpha)} \frac{d^m}{dt^m} \int_0^t \frac{\theta(\tau) d\tau}{(t-\tau)^{\alpha-m+1}}, \quad m-1 < \alpha \leq m, \end{aligned}$$

$$\begin{aligned} {}_0^C D_t^\alpha \theta(t) &= {}_0\mathcal{I}_t^{m-\alpha} D_t^m \theta(t) \\ &= \frac{1}{\Gamma(m-\alpha)} \int_0^t \frac{D_t^m \theta(\tau) d\tau}{(t-\tau)^{\alpha-m+1}}, \quad m-1 < \alpha \leq m, \end{aligned}$$

with $D_t^m = d^m/dt^m$, ${}_0\mathcal{I}_t^m f(t)$ is a fractional integral given by

$${}_0\mathcal{I}_t^m f(t) = \frac{1}{\Gamma(m)} \int_0^t (t-\tau)^{\alpha-1} f(\tau) d\tau,$$

and Γ is the Gamma function.

All the fKRs listed above, have stroboscopic versions which are two-dimensional nonlinear maps with memory given in action-angle variables (I, θ) . These maps are named as fractional standard maps (fSMs), in resemblance with Chirikov's standard map (CSM) [11]:

$$\begin{aligned} I_{n+1} &= I_n - K \sin(\theta_n), \\ \theta_{n+1} &= \theta_n + I_{n+1}, \quad \text{mod}(2\pi); \end{aligned} \quad (4)$$

which is the stroboscopic version of the standard kicked rotor of Eq. (1). Here and below, T is set to one.

As far as we know, the first two fSMs reported in the literature are the Riemann-Liouville fSM (RL-fSM) [2, 3],

$$\begin{aligned} I_{n+1} &= I_n - K \sin(\theta_n), \\ \theta_{n+1} &= \frac{1}{\Gamma(\alpha)} \sum_{i=0}^n I_{i+1} V_\alpha^1(n-i+1), \quad \text{mod}(2\pi), \end{aligned} \quad (5)$$

and the Caputo fSM (C-fSM) [4, 5],

$$\begin{aligned} I_{n+1} &= I_n \\ &\quad - \frac{K}{\Gamma(\alpha-1)} \left[\sum_{i=0}^{n-1} V_\alpha^2(n-i+1) \sin(\theta_i) + \sin(\theta_n) \right], \\ \theta_{n+1} &= \theta_n + I_0 \\ &\quad - \frac{K}{\Gamma(\alpha)} \sum_{i=0}^n V_\alpha^1(n-i+1) \sin(\theta_i), \quad \text{mod}(2\pi). \end{aligned} \quad (6)$$

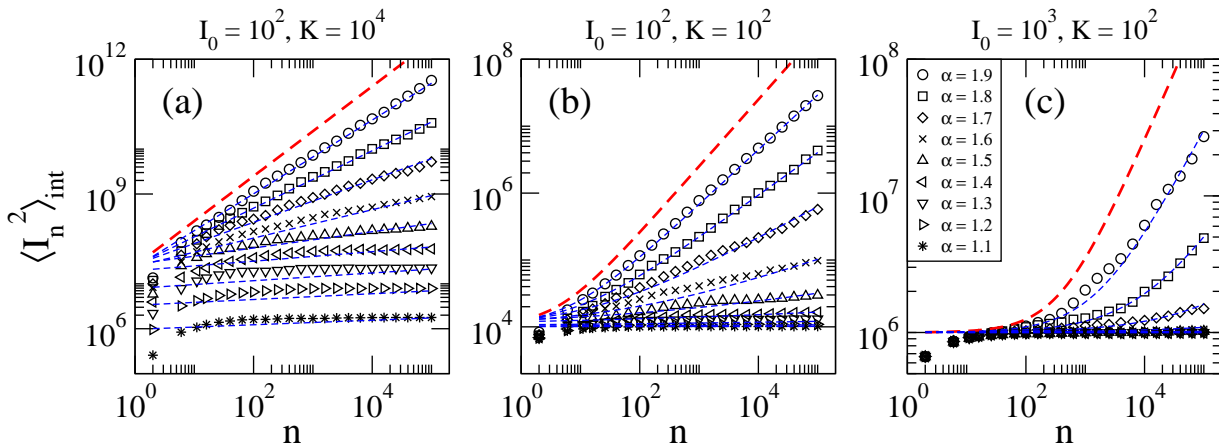


FIG. 1: Average squared action $\langle I_n^2 \rangle_{\text{int}}$ as a function of n for (a) $(I_0, K) = (10^2, 10^4)$, (b) $(I_0, K) = (10^2, 10^2)$, and (c) $(I_0, K) = (10^3, 10^2)$. Several values of α are considered, as indicated in panel (c). Red-dashed lines correspond to Eq. (7). Blue-dashed lines are Eq. (10). The average is taken over $M = 200$ orbits with initial random phases in the interval $0 < \theta_0 < 2\pi$.

Here, $1 < \alpha \leq 2$ is assumed and

$$V_\alpha^k(m) = m^{\alpha-k} - (m-1)^{\alpha-k}.$$

Both, the RL-fSM and the C-fSM are parameterized by K and α which control the strength of nonlinearity and the fractional order of the derivative, respectively. For $\alpha = 2$, both the RL-fSM and the C-fSM reproduce the CSM [5, 11].

As compared with the CSM, which presents the generic transition to chaos (in the context of Kolmogorov–Arnold–Moser theorem, see e.g. [1]), depending on the parameter pair (K, α) , the RL-fSM and the C-fSM show richer dynamics: They generate attractors (fixed points, asymptotically stable periodic trajectories, slow converging and slow diverging trajectories, ballistic trajectories, and fractal-like structures) and/or chaotic trajectories [3, 5, 12, 13].

Among several available studies on the RL-fSM and the C-fSM (see e.g. [3, 5, 12, 13]), very recently, the squared average action $\langle I_n^2 \rangle$ of the RL-fSM was analyzed in the regime of $K \gg 1$ [14]. There it was shown that, for strongly chaotic orbits, $\langle I_n^2 \rangle$ presents normal diffusion (for sufficiently large times) and, in addition, it does not depend on α . Indeed, the panorama reported for $\langle I_n^2 \rangle$ vs. n for the RL-fSM [14] is equivalent to that of the CSM [15, 16] as well as that of the discontinuous standard map (DSM) [15, 17], both with $K \gg 1$. Moreover, an analytical estimation [14], used to get

$$\langle I_n^2 \rangle_{\text{RL-fSM}} = I_0^2 + \frac{K^2}{2}n, \quad (7)$$

also showed the independence of $\langle I_n^2 \rangle$ on α .

By following the derivation of Eq. (7) we have realized that the independence of $\langle I_n^2 \rangle$ on α is due to the absence of α in the first equation of map (5). That is way Eq. (7) also describes the dynamics of CSM: note that the equation for the action is the same in both maps; see

Eqs. (4) and (5). This suggests that $\langle I_n^2 \rangle$ may depend on α in fractional maps where α appears in the equation for the action, such as map (6). Unfortunately, by the use of simple arguments as those used to get Eq. (7) in Ref. [14], we are not able to get an explicit expression for $\langle I_n^2 \rangle$ for the C-fSM.

Therefore, the purpose of this work is twofold. First, we numerically look for the effects of α on $\langle I_n^2 \rangle$ for the C-fSM, $\langle I_n^2 \rangle_{\text{C-fSM}}$. Second, we derive a phenomenological expression for $\langle I_n^2 \rangle_{\text{C-fSM}}$ which properly incorporates the parameter α .

II. ON THE EFFECTS OF α ON $\langle I_n^2 \rangle_{\text{C-fSM}}$

To ease our numerical analysis, to get curves smoother than the present $\langle I_n^2 \rangle_{\text{C-fSM}}$ vs. n , in what follows we compute the cumulative-normalized value of $\langle I_n^2 \rangle_{\text{C-fSM}}$,

$$\langle I_n^2 \rangle_{\text{int}} = \frac{1}{n} \int_{n_0=0}^n \langle I_{n'}^2 \rangle_{\text{C-fSM}} dn',$$

by averaging over M independent orbits (by randomly choosing values of θ_0 in the interval $0 < \theta_0 < 2\pi$) for each combination of parameters (I_0, K, α) .

Then, in Fig. 1 we plot $\langle I_n^2 \rangle_{\text{int}}$ as a function of n for the C-fSM for several values of α in the interval $1 < \alpha < 2$. Moreover, in all panels we include Eq. (7) (as red-dashed curves) which corresponds to the case $\alpha = 2$; so we can contrast the results for the C-fSM with those for the RL-fSM [14], the CSM [15, 16], and the DSM [15, 17]. In Fig. 1 we use three representative parameter pairs (I_0, K) : $I_0 < K$ (left panel), $I_0 = K$ (central panel), and $I_0 > K$ (right panel).

From Fig. 1 we can clearly observe that α suppresses the action diffusion even at the very first iteration; moreover, the smaller the value of α the larger the difference

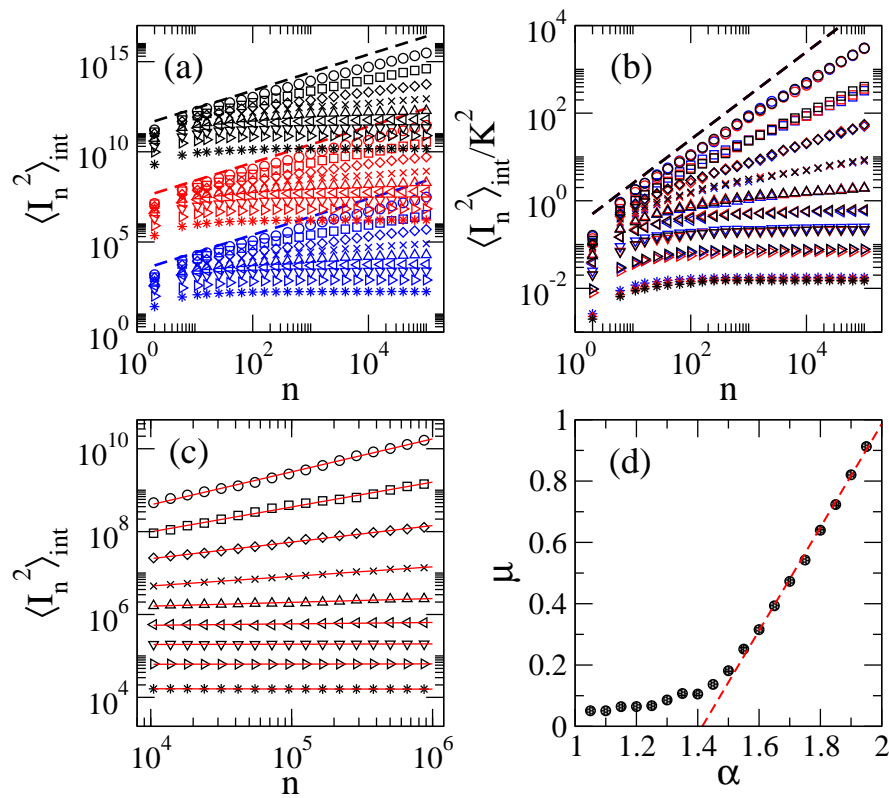


FIG. 2: (a) Average squared action $\langle I_n^2 \rangle_{\text{int}}$ as a function of n for $K = 10^2$ (blue symbols), $K = 10^4$ (red symbols), and $K = 10^6$ (black symbols). In all cases $I_0 = 0$. The average is taken over $M = 200$ orbits with initial random phases in the interval $0 < \theta_0 < 2\pi$. Several values of α are considered; same symbol labeling as in Fig. 1. Dashed lines correspond to Eq. (7). (b) $\langle I_n^2 \rangle_{\text{int}} / K^2$ vs. n . Same data as in panel (a). (c) $\langle I_n^2 \rangle_{\text{int}}$ vs. n for $K = 10^3$ and $I_0 = 0$. Here the average is taken over $M = 100$ orbits with initial random phases in the interval $0 < \theta_0 < 2\pi$. Dashed lines correspond to power-law fittings of the form $\langle I_n^2 \rangle_{\text{int}} \propto n^\mu$ in the interval $n = [10^4, 10^6]$. (d) μ , from the power-law fittings of panel (c), as a function of α . The red-dashed line is a linear fit to the data with $\alpha > 0.5$: $\mu \sim 1.69\alpha$.

between $\langle I_n^2 \rangle_{\text{int}}$ and the red-dashed curves which correspond to normal diffusion. Also, for large iteration times $\langle I_n^2 \rangle_{\text{int}}$ grows proportional to n^μ with $\mu \equiv \mu(\alpha)$; this can be better observed in Fig. 1(a). In addition, we observe two scenarios depending on the initial action I_0 as compared with K . Specifically, when $I_0 < K$, the curves $\langle I_n^2 \rangle_{\text{int}}$ vs. n are all different for different α and approach faster the regime $\langle I_n^2 \rangle_{\text{int}} \propto n^\mu$; see e.g. Fig. 1(a). While for $I_0 > K$, first, the curves $\langle I_n^2 \rangle_{\text{int}}$ vs. n for different α fall one on top of the other up to a crossover time n^* , after which $\langle I_n^2 \rangle_{\text{int}}$ grows proportional to n^μ ; see e.g. Fig. 1(c).

In what follows we concentrate on the case $I_0 < K$ to easily approach the asymptotic regime where $\langle I_n^2 \rangle_{\text{int}} \propto n^\mu$. So, in Fig. 2(a) we show $\langle I_n^2 \rangle_{\text{int}}$ as a function of n for several values of α and $I_0 = 0$. Here we have used three values of K : $K = 10^2$ (blue symbols), $K = 10^4$ (red symbols), and $K = 10^6$ (black symbols). Note that the contribution of K to $\langle I_n^2 \rangle_{\text{int}}$ is through the factor K^γ , i.e. $\langle I_n^2 \rangle_{\text{int}} \propto K^\gamma n^\mu$, where γ should be equal to 2, see e.g. Eq. (7). We verify this last statement in Fig. 2(b) where we plot the same curves of panel (a) but now divided by K^2 and observe that curves for the same α fall

one on top of the other.

Then, to characterize the dependence of μ on α in the asymptotic regime, i.e. where $\langle I_n^2 \rangle_{\text{int}} \propto n^\mu$, in Fig. 2(c) we look at large iteration times. There, we perform power-law fittings of the form $\langle I_n^2 \rangle_{\text{int}} \propto n^\mu$ in the interval $n = [10^4, 10^6]$. The values of μ obtained from the fittings are reported in Fig. 2(d). From Fig. 2(d) we can see that $\mu \rightarrow 0$ for $\alpha \rightarrow 1$ while $\mu \rightarrow 1$ for $\alpha \rightarrow 2$. In addition we observe that $\mu(\alpha) \propto \alpha$ for $\alpha > 0.5$.

Indeed, by substituting $\alpha = 1$ into Eq. (6), since $\Gamma(0)$ diverges the action remains constant, $I_n = I_0$, so the action diffusion is fully suppressed and $\mu(\alpha = 1) = 0$. While substituting $\alpha = 2$ into map (6), since $\Gamma(1) = 1$ and $V_2^2(m) = 0$, the equation for to action reduces to $I_{n+1} = I_n - K \sin(\theta_n)$; so $\langle I_n^2 \rangle$ is described by Eq. (7) and $\mu(\alpha = 2) = 1$. Therefore, for $1 < \alpha < 2$ the C-fSM shows subdiffusion:

$$\langle I_n^2 \rangle_{\text{int}} \propto K^2 n^{\mu(\alpha)} \quad \text{with} \quad 0 < \mu(\alpha) < 1, \quad (8)$$

which can be observed for large enough n .

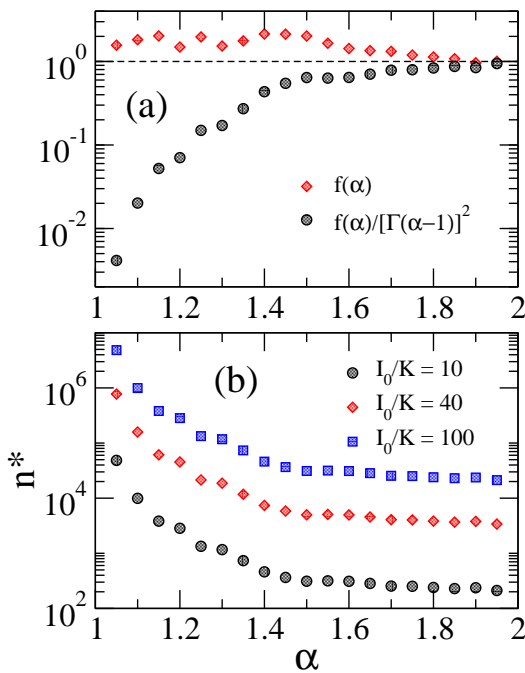


FIG. 3: (a) $f(\alpha)$ and $f(\alpha)/[\Gamma(\alpha-1)]^2$. $f(\alpha)$ is obtained from the power-law fittings of the form $\langle I_n^2 \rangle_{\text{int}} = Cn^\mu$ to the data of Fig. 2(c); i.e. $f(\alpha) = 2C[\mu(\alpha)+1][\Gamma(\alpha-1)]^2/K^2$, here with $K = 10^3$. (b) $n^*(\alpha)$ for three ratios I_0/K ; see Eq. (14).

III. HEURISTIC ESTIMATE OF $\langle I_n^2 \rangle_{\text{C-fSM}}$

In analogy with Eq. (7) and taking into account the scaling given in Eq. (8), we surmise

$$\langle I_n^2 \rangle_{\text{C-fSM}} = I_0^2 + \frac{K^2}{2} \frac{f(\alpha)}{[\Gamma(\alpha-1)]^2} n^{\mu(\alpha)}, \quad (9)$$

which leads to

$$\langle I_n^2 \rangle_{\text{int}} = I_0^2 + \frac{K^2}{2} \frac{f(\alpha)}{[\Gamma(\alpha-1)]^2 [\mu(\alpha)+1]} n^{\mu(\alpha)}. \quad (10)$$

Indeed, from the power-law fittings made in Fig. 2(c) we can extract $f(\alpha)$, which is plotted in Fig. 3(a). Notice that $f(\alpha) \sim 2$ for $\alpha < 0.5$, while it tends to one for $\alpha \rightarrow 2$, as expected. In Fig. 3(a) we also plot the ratio $f(\alpha)/[\Gamma(\alpha-1)]^2$, which is relevant since it appears in Eq. (9) and together with the power $\mu(\alpha)$ is one of the key differences between this equation and Eq. (7) for the RL-fSM.

In Fig. 1 we include Eq. (10), as blue-dashed lines and observe a reasonable good correspondence with the data. We believe that the correspondence between Eq. (10) and the data should improve by increasing the number of orbits used in the computation of $\langle I_n^2 \rangle_{\text{int}}$. Moreover, we also note an important deviation of the data from Eq. (10) for very short times, $n < 10$, where Eq. (10) completely fails.

IV. DISCUSSION AND CONCLUSIONS

It is relevant to note that Eq. (9) can be used to define an effective parameter controlling the strength of nonlinearity K_{eff} in the C-fSM as

$$\langle I_n^2 \rangle_{\text{C-fSM}} = I_0^2 + \frac{K_{\text{eff}}^2(\alpha)}{2} n^{\mu(\alpha)}, \quad (11)$$

with

$$K_{\text{eff}}(\alpha) \equiv \frac{\sqrt{f(\alpha)}}{\Gamma(\alpha-1)} K. \quad (12)$$

Indeed, the form of Eq. (11) is very convenient because allows a direct comparison with Eq. (7) which describes the squared average action of the RL-fSM but also of the CSM and the DSM. Thus, it is relevant to stress that, since $K_{\text{eff}}(\alpha) \propto 1/\Gamma(\alpha-1)$, $K_{\text{eff}} \rightarrow 0$ for $\alpha \rightarrow 1$ while $K_{\text{eff}} \rightarrow K$ for $\alpha \rightarrow 2$.

Moreover, from the ratio

$$\frac{\langle I_n^2 \rangle_{\text{C-fSM}}}{I_0^2} = 1 + \frac{n^\mu}{n^*}, \quad (13)$$

we can identify the crossover time

$$n^*(I_0, K, \alpha) \equiv 2 \frac{I_0^2}{K_{\text{eff}}^2} = 2 \frac{I_0^2}{K^2} \frac{[\Gamma(\alpha-1)]^2}{f(\alpha)}. \quad (14)$$

Notice also that Eq. (11) allow us to define the scaling laws

$$\langle I_n^2 \rangle_{\text{C-fSM}} = \begin{cases} \propto K_{\text{eff}}^2 n^\mu, & \text{when } I_0 \ll K_{\text{eff}}, \\ \approx I_0^2, & n < n^* \\ \propto K_{\text{eff}}^2 n^\mu, & n > n^* \end{cases} \quad \text{when } I_0 \gg K_{\text{eff}}. \quad (15)$$

Here, n^* separates the regime of constant action and the subdiffusive regime when $I_0 \gg K_{\text{eff}}$. However, note that since $n^* \propto [\Gamma(\alpha-1)]^2$, and $\Gamma(\alpha-1)$ diverges for $\alpha \rightarrow 1$, in practice, the subdiffusive regime may never be approached for $\alpha \rightarrow 0$. As examples, in Fig. 3(b) we plot $n^*(\alpha)$ for three ratios I_0/K . Notice that for $\alpha \sim 1.05$ and $I_0/K = 100$, n^* is already of the order of 10^7 .

Finally, it is relevant to recall that subdiffusive dynamics has already been reported for the CSM, see e.g. [18–20]. Specifically, $\mu = 0.9$ [18] and $\mu = 0.25$ [19] were found for the CSM with $K = 7$ and $K = 1.46$, respectively. However, the anomalous diffusion shown in Refs. [18–20] is produced by stickiness around islands of stability in a mixed phase space. In contrast, the mechanism for the anomalous diffusion we report here is completely different: Anomalous diffusion in the C-fSM is a consequence of the memory, imposed by the Caputo fractional derivative, in the equation for the action.

Given that subdiffusion in the C-fSM can continuously be tuned with the parameter α (from weak subdiffusion, $\mu \sim 1$, to strong subdiffusion, $\mu \sim 0$), the C-fSM may serve as a reference model to prove and characterize the effects of subdiffusion in other dynamical properties of interest, such as scattering and transport properties.

Acknowledgements

J.A.M.-B. thanks support from CONAHCyT-Fronteras (Grant No. 425854) and VIEP-BUAP (Grant

No. 100405811-VIEP2024), Mexico.

-
- [1] E. Ott, *Chaos in dynamical systems* (Cambridge Univ. Press, 2008).
- [2] V. E. Tarasov and G. M. Zaslavsky, Fractional equations of kicked systems and discrete maps, *J. Phys. A* **41**, 435101 (2008).
- [3] M. Edelman and V. E. Tarasov, Fractional standard map, *Phys. Lett. A* **374**, 279–285 (2009).
- [4] V. E. Tarasov, Differential equations with fractional derivative and universal map with memory, *J. Phys. A* **42**, 465102 (2009).
- [5] M. Edelman, Fractional standard map: Riemann-Liouville vs. Caputo, *Commun. Nonlinear. Sci. numer. Simulat.* **16**, 4573–4580 (2011).
- [6] V. E. Tarasov, Fractional dynamics with non-local scaling, *Commun. Nonlinear Sci. Numer. Simulat.* **102**, 105947 (2021).
- [7] V. E. Tarasov, Nonlinear fractional dynamics with kicks, *Chaos Solitons Fractals* **151**, 111259 (2021).
- [8] V. E. Tarasov, From fractional differential equations with Hilfer derivatives to discrete maps with memory, *Com. Appl. Math.* **40**, 296 (2021).
- [9] S. G. Samko, A. A. Kilbas, and O.I. Marichev, *Fractional integrals and derivatives. Theory and applications* (Gordon and Breach, New York, 1993).
- [10] A. A. Kilbas, H. M. Srivastava, and J. J. Trujillo, *Theory and application of fractional differential equations* (Elsevier, Amsterdam, 2006).
- [11] B. V. Chirikov, Research concerning the theory of nonlinear resonance and stochasticity, Preprint 267, Institute of Nuclear Physics, Novosibirsk (1969). *Engl. Trans., CERN Trans.* (1971) 71-40.
- [12] M. Edelman and L. A. Taieb, New types of solutions of non-linear fractional differential equations, in *Advances in Harmonic Analysis and Operator Theory; Series: Operator Theory: Advances and Applications*, A. Almeida, L. Castro, F.-O. Speck (Eds.) (Springer, Basel, 2013), pp. 139–155.
- [13] M. Edelman, Dynamics of nonlinear systems with power-law memory, in *Volume 4 Applications in Physics, Part A, Handbook of fractional calculus with applications*, V. E. Tarasov (Ed.) (De Gruyter, Berlin, Boston, 2019) pp. 103–132.
- [14] J. A. Mendez-Bermudez, R. Aguilar-Sanchez, J. M. Sigarreta, and E. D. Leonel, Scaling properties of the action in the Riemann-Liouville fractional standard map, arXiv:2402.17673.
- [15] J. A. Mendez-Bermudez, J. A. deOliveira, and E. D. Leonel, Analytical description of critical dynamics for two-dimensional dissipative nonlinear maps, *Phys. Lett. A* **380**, 1959 (2016).
- [16] D. G. Ladeira and J. K. L. da Silva, Scaling properties of a simplified bouncer model and of Chirikov’s standard map, *J. Phys. A: Math. Theor.* **40**, 11467 (2007).
- [17] J. A. Mendez-Bermudez and R. Aguilar-Sanchez, Scaling properties of discontinuous maps, *Phys. Rev. E* **85**, 056212 (2012).
- [18] T. Manos and M. Robnik, Dynamical localization in chaotic systems: Spectral statistics and localization measure in the kicked rotator as a paradigm for time-dependent and time-independent systems, *Phys. Rev. E* **87**, 062905 (2013).
- [19] M. S. Palmero, G. I. Diaz, I. L. Caldas, and I. M. Sokolov, Sub-diffusive behavior in the standard map, *Eur. Phys. J. Spec. Top.* **230**, 2765–2773 (2021).
- [20] H. T. Moges, T. Manos, and C. Skokos, Anomalous diffusion in single and coupled standard maps with extensive chaotic phase spaces, *Physica D* **431**, 133120 (2022).